01 Feb 2022

Flow Regimes in Gas-Solid Fluidized Beds Via Micro-Foil Heat Flux Sensor

Haidar Taofeeq

Sebastián Uribe

Muthanna H. Al-Dahhan
Missouri University of Science and Technology, aldahhanm@mst.edu

Recommended Citation

H. Taofeeq et al., "Flow Regimes in Gas-Solid Fluidized Beds Via Micro-Foil Heat Flux Sensor," *Chemical Engineering and Technology*, vol. 45, no. 2, pp. 220 - 229, Wiley; Gesellschaft Deutscher Chemiker; Gesellschaft für Chemische Technik und Biotechnologie, Feb 2022.
The definitive version is available at https://doi.org/10.1002/ceat.202000559

Haidar Taofeeq[1,2]
Sebastián Uribe[3]
Muthanna Al-Dahhan[3,*]

Flow Regimes in Gas-Solid Fluidized Beds via Micro-Foil Heat Flux Sensor

The flow regime transitions in a gas-solid fluidized bed were studied for the first time using a micro-foil heat flux sensor. The time series of heat flux signals was analyzed by statistical and state space methods. The experimental measurements were performed in a lab-scale gas-solid fluidization column. Four different flow regimes, i.e., fixed-bed flow regime, bubbling-flow regime, slugging-flow regime, and turbulent-flow regime, and three intermediate transition velocities, i.e., minimum fluidizing velocity or minimum bubbling velocity, minimum slugging velocity, and minimum turbulent velocity, were successfully identified. The method based on the analysis of heat flux sensor measurements allowed to determine accurately the different flow regimes and the transition velocities.

Keywords: Flow regimes, Gas-solid fluidized beds, Micro-foil heat flux sensors, Transition velocities

Received: November 23, 2020; *revised:* November 20, 2021; *accepted:* November 22, 2021

DOI: 10.1002/ceat.202000559

1 Introduction

Gas-solid fluidized beds (FBs) are multiphase reactors, where fine solids particles are suspended and fluidized by the upward flow of the gas phase at high velocities. This characteristic multiphase flow and interaction phenomena allow these reactors to have high mass and heat transfer rates due to the high gas-solid contact and intense solids mixing, as well as nearly isothermal temperature distributions even for highly exothermic reactions, and low pressure drops [1, 2]. In fact, the high heat transfer rate is considered one of the most important characteristics of gas-solid fluidized beds, which makes these systems highly desirable and recommended for industrial applications.

Nevertheless, a deep understanding of the hydrodynamics and heat transfer on the gas-solid fluidized bed is still a major challenge. To a great extent, the lack of a deeper knowledge of the local-scale phenomena on FBs lies in the complexity of the multiphase and multiscale interactions, and the recognized scale dependency of these systems [2, 3]. Remarkably, it has been reported in the literature that the gas-phase dynamics are strongly scaled dependent and are deeply affected by textural characteristics of the bed, such as the column diameter to average solid particle diameter ratio (D_C/d_p)[1)], the solid particles material and size, and the presence of internal structures, or even the walls of the vessel [4–7]. This disadvantageous characteristic of the hydrodynamic behavior of FBs affects important design parameters, such as bubble size, bubble rise velocity, bubble trajectories, and bubble growth, hence, altering the radial dispersion of the bubbling gas phase [3]. For reactive fluidized beds, these phenomena in the gas phase will influence the mass transfer of reactants from the bubbling gas phase to the disperse solids phase, thus, affecting the reactor throughput and its thermal behavior [2].

In other words, the gas and solid flow patterns are impacted by several complex and intricate interactions inside the bed, which end up altering the flow regime, and thus, the transition velocities. Therefore, further research efforts to understand the influence of the interaction phenomena between the solids, gas, immersed internals, and the wall of the vessel over the flow regimes and their transition velocities in gas-solid fluidized beds are yet required.

In this context, Taofeeq and Al-Dahhan [8] reviewed several techniques used to estimate the flow regimes in gas-solid fluidized beds, such as pressure transducer, high-speed camera, optical fiber probe, γ-ray densitometry, and fast X-ray tomography. They analyzed the factors that influence the flow regime in such systems, such as design parameters, physical properties of gas and solids, and operation conditions. Also, they compared different methods of analysis that can be applied to the collected data from these techniques to estimate the flow

1) List of symbols at the end of the paper.

[1]Dr. Haidar Taofeeq
Chemical Engineering Department, College of Engineering, Al-Nahrain University, Baghdad, Iraq.

[2]Dr. Haidar Taofeeq
Prosthetics and Orthotics Engineering Department, College of Engineering, Al-Nahrain University, Baghdad, Iraq.

[3]Sebastián Uribe, Prof. Muthanna Al-Dahhan
aldahhanm@mst.edu
Department of Chemical and Biochemical Engineering, Missouri University of Science and Technology, Rolla, MO, 65409, USA.

regimes and transition velocities, such as flow regime mapping, time-domain analysis, frequency domain analysis, and state space analysis. In this broad review [8], the authors were able to identify the effect of the presence of vertical internals of two different diameters (0.0127 and 0.0254 m) that mimicked heat exchangers, as well as the effect of different particle materials (glass beads and aluminum oxide) with different physical properties, over the flow regimes and their transition velocities. The identification of the different flow regimes was conducted by investigating the pressure fluctuations collected from a differential pressure transducer, using state space analysis (Kolmogorov entropy) and time-domain analysis (standard deviation).

Several other works found in the literature regarding the application of different experimental and analysis techniques can be highlighted. Kalo et al. [9] studied the flow regime in a conical gas-solid fluidized bed using mono and binary solid particles. The flow regimes were identified using the Kolmogorov entropy approach applied to the time series of radioactive particle tracking (RPT) technique data. Zhou et al. [10] paired acoustic emission and a pressure transducer to explore the flow regime transition process in a circulating gas-solid two-phase fluidization system.

Hamidifard et al. [11] studied the flow regime and hydrodynamics phenomena of a fluidized bed packed with Geldart B sliver oxide nanoparticle agglomerates through experimental and numerical methods. The experimental measurements were carried out in a bench-scale Plexiglas fluidized bed of 0.06 m inside diameter. They applied optical fiber probe and pressure transducer techniques to study the hydrodynamic behavior and flow regime. To investigate the fluidizing system numerically, they implemented a Eulerian-Eulerian model (TFM) and found a reasonably good agreement between the simulated and experimentally determined different flow regimes (fixed bed, bubbling, slugging, and turbulent flow regime) and the hydrodynamics behavior of the system.

Zhu et al. [12] studied the flow regime of a magnetized fluidized bed with Geldart B particles using visual observation in terms of camera and multichannel pressure transducers. Boonprasop et al. [13] investigated the flow regime in a circulating fluidized-bed system, using pressure sensors at eight different points along the riser section of the bed. The pressure fluctuation signals were collected and analyzed to present a new flow regime diagram, which considers the effects of both the design parameters and operating conditions.

Yang et al. [14] identified the transition velocities in a vertical pneumatic conveying by analyzing the acoustic and electrostatic signals along with a pressure sensor. From their results, they were able to obtain two flow regime maps, which accounted for the relation between acoustic energy and pressure drop, and between electrostatic accumulation and pressure drop.

As can be noted, the identification of the flow regimes transitions strongly relies on the analysis of the pressure fluctuations and other invasive techniques, such as the application of optical fiber sensors. The main drawback of relying on the analysis of pressure fluctuations is that the absolute and differential pressure transducers are usually located in ports mounted on the vessel wall along with the column height, which means that the measurements correspond to limited locations found away from the core of the fluidized bed. Thus, to obtain detailed insights into the effect of internal structures, such as heat exchange tubes, over the flow regimes in fluidized beds, there is still a need to develop a different methodology to capture the gas and solids interactions with the internal walls.

Considering such needs, the objective of the present study is to use a micro-foil heat flux sensor for the first time to identify the flow regime transitions in a laboratory-scale gas-solid fluidized bed. This micro-foil sensor is flush-mounted on a wall of the internals in a non-invasive way and can measure the time-wise heat flux and surface temperature at such a specific location. Accordingly, the present methodology is based on analyzing the micro-foil sensor's voltage signal using the time domain method (standard deviation) and the state space method (Kolmogorov entropy).

2 Experimental Setup

The details of the experimental setup used in this work have been reported in the authors' previous contributions [8, 15–18]. The lab-scale fluidized-bed setup consists of a 0.14-m inside diameter column of 1.84 m in height made of Plexiglas. The plenum section under the column was built from aluminum, which was placed on a stainless-steel base. Compressed air at room temperature was fed to the plenum through a sparge tube. The T-shaped sparge tube has 14 holes facing downwards to improve the air distribution in the plenum section. The plenum and the column sections were connected with a porous polyethylene sheet with a pore size of around 15–40 μm. To minimize electrostatic-charge effects, the column was electrically grounded with a copper wire mesh, and to minimize the mechanical vibrations, the column was placed on a rigid metallic structure. A schematic diagram of the experimental setup can be seen in Fig. 1, and Fig. 2 presents a picture of the experimental setup on our facilities. Further details of the construction can be found elsewhere [8, 15–18].

The gas phase introduced through the sparge tube was compressed air. Industrial-scale compressors installed in the facilities, which reach up to 1.38 MPa, were used. Pressure stabilizers were used to regulate the inlet pressure to the flowmeters that control the air inflow to the column, and which are calibrated at 0.69 MPa. With the described configuration, the air inflow to the plenum was found close to atmospheric pressure and room temperature.

The experimental measurements were conducted at superficial gas inlet velocities between 0.35 and 1.1 m s^{-1}. The range of superficial gas inlet velocities was selected to ensure that the bed operates at different flow regimes (fixed-bed, bubbling, slugging, and turbulent-flow regime) as identified by Taofeeq [6] and Taofeeq and Al-Dahhan [8, 16].

The heat transfer measurements were acquired at the center of the bed, corresponding to the radial position of $r/R = 0$, and at an axial position of $H/D = 1.5$ above the gas distributor. Such location represents the middle region of the fluidized-bed column. To place the micro-foil heat flux sensor, a rod was inserted from the top of the column, representing a vertical internal.

Geldart B glass beads of an average diameter of 365 μm, sphericity of 0.9, and a density of 2500 kg m^{-3} were used in the

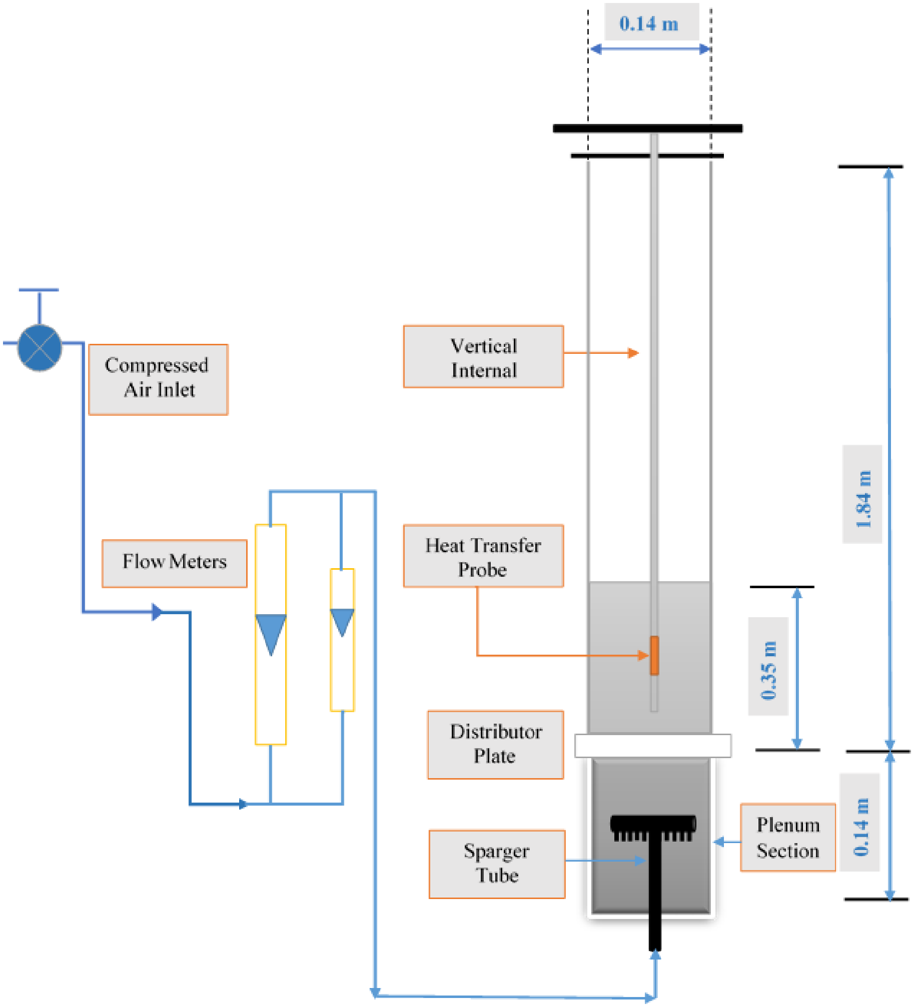

Figure 1. Schematic diagram of 0.14 m inside diameter bench-scale fluidized-bed column used in the present work.

experimental study. The actual particle size was found to have a distribution between 300 and 430 μm. The column was initially packed to a static bed height of 0.35 m.

Under similar conditions, using the same experimental setup and solid particles, in a previous study, the minimum fluidizing velocity was measured to be 0.4 m^{-1}s [6, 16]. Such experiments were conducted with a differential pressure transducer. Such minimum fluidizing velocity remained the same for this study since the same solid particles, static bed height, and column diameter were employed. Further details regarding the minimum fluidizing velocity measurement can be found in Taofeeq and Al-Dahhan [16].

3 Advanced Heat Transfer Probe Technique

To measure the heat flux voltage signals, a brass cylinder, where a heat transfer probe was flush-mounted, was placed on an internal vertical rod. Such a rod was inserted in the FB column in the center of the column, as demonstrated in Fig. 1. The micro-foil sensor has a dimension of 0.0254 m in width and a length of 0.095 m, which allows it to be flush-mounted on different surfaces in a non-invasive way. The heat transfer probe enables to locally measure in a non-invasive way with high accuracy the local heat flux and surface temperature. It allows recording fast response time series fluctuations of such measurements. Details of the heat transfer probe on the internal rod can be seen in Fig. 3.

The heat transfer probe technique has been used to determine the local heat transfer coefficient in several multiphase flow systems, such as gas-solid fluidized beds, bubble columns, and other heat transfer systems [19–25]. In these works, the measured heat flux and surface temperature obtained from the heat transfer probe were used to determine the local heat transfer coefficient and its local variations, such as axial and radial profiles.

To mimic the phenomena occurring in a heat exchanger tube, a heating cartridge (Chromalox, model CIR-1012) was placed inside the brass cylinder on the vertical internal rod. The heat flux was supplied by the heating cartridge and transported through the brass cylinder, and the brass cylinder surface temperatures were simultaneously measured by the sensor. A voltage amplifier (JH Technology, Inc., model JH4300) was used to pre-process the micro-volt response measured by the sensor. The amplified signal was then received by a data acquisition system (DAQ, model NI-9205). Heat flux measurements were recorded for 100 s at a 100-Hz sampling rate, using LabVIEW. All experiments were repeated three times to ensure the reproducibility of the results and to determine error bars. The deviations between the repetitions were found to be less than 5 %.

4 Data Analysis Methods

4.1 Statistical Analysis (Standard Deviation)

One of the most common methods to identify the different flow regimes in FBs is the analysis of standard deviations [9, 12, 26–28]. In this method, the standard deviation of a timewise sampled metric at different superficial gas inlet velocities is estimated. Then, the change of the standard deviation against increasing superficial inlet velocity is observed. In this

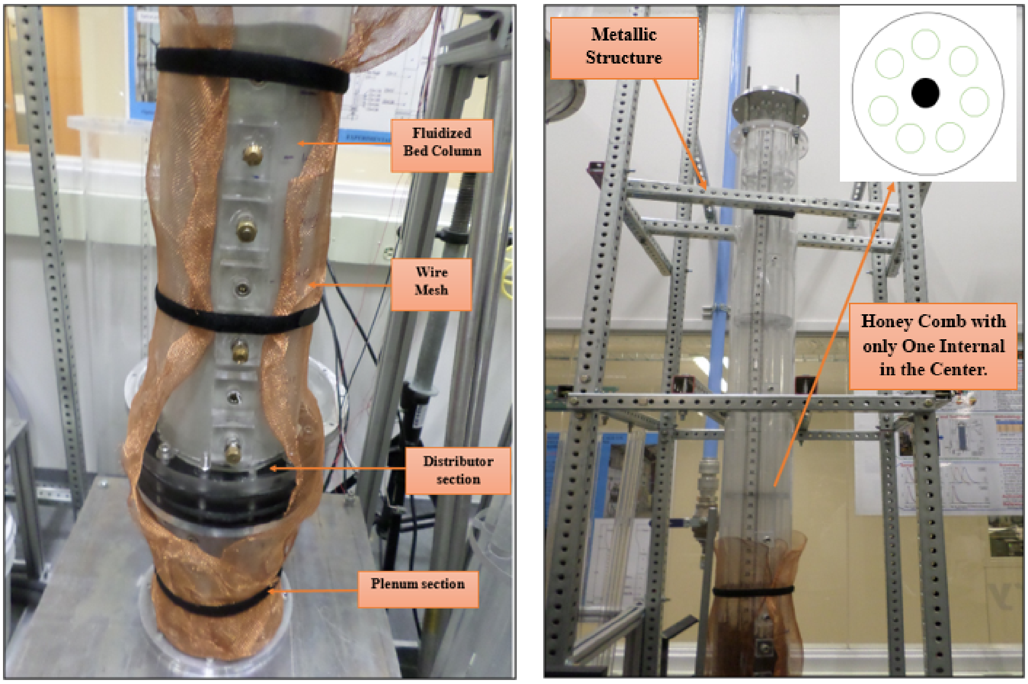

Figure 2. Photos of the fluidized-bed column with metallic structure and copper wire mesh.

series, local maximums in the standard deviations are identified, which indicates that such superficial gas inlet velocity corresponds to a transition velocity [29].

To apply the standard deviation method in the current methodology, the measured heat flux by the sensor can be considered as the metric. The standard deviation of the heat flux signal at different superficial inlet velocities was estimated to identify the different transition velocities and flow regimes. In this way, the estimated standard deviation in the measured heat flux response signal will increase when raising the superficial gas inlet velocity until it reaches a local maximum. After such a local maximum, the estimated standard deviation will decrease, and then at higher superficial gas inlet velocities it will increase again until another local maximum is found, which will correspond to a new flow regime transition or to another flow structure within the same flow regime. In a previous contribution, the same behavior was observed when analyzing the pressure fluctuation signals measured by a differential pressure transducer [18].

The standard deviation (SD) of the heat flux time series was calculated according to the following equation:

$$\mathrm{SD} = \sqrt{\frac{\sum_{\mathrm{i}=1}^{\mathrm{N}} (x_{\mathrm{i}} - \bar{x})^2}{(N-1)}} \quad (1)$$

where x_{i} represents each timewise measurement, N is the total number of the data points (which is 10 000), and $\bar{x}$ is the mean of the time series, calculated according to Eq. (2):

$$\bar{x} = \frac{\sum_{\mathrm{i}=1}^{\mathrm{N}} x_{\mathrm{i}}}{N} \quad (2)$$

4.2 State Space Analysis (Kolmogorov Entropy)

FBs have been recognized as systems of chaotic dynamic behavior, which arise from the intricate multiphase interactions, and the effect of the surroundings over the gas-phase dynamics, such as wall effects from the gas-wall interactions, or the interaction with internal surfaces. Consequently, the degree of disorder in the system is a function of vast multiphase hydrodynamic parameters, such as the phases holdups and velocities, turbulence variables, as well as bubble dynamics parameters (bubble size, frequency, and velocity).

To characterize such chaotic behavior of FBs, several methodologies have been proposed and applied in literature, such as attractor reconstruction, correlation dimension, entropy, and the Kolmogorov entropy (KE). Among these methodologies, the KE analysis has been recognized as one of the most insightful methodologies to characterize the chaotic behavior of FBs, according to Van Ommen et al. [29, 30]. Thus, KE was selected in this work for estimating the chaotic degree in the studied FB.

KE was calculated based on the maximum likelihood estimation of entropy, as described by Schouten et al. [31] and Nedeltchev et al. [32, 33]:

$$\mathrm{KE} = -f_{\mathrm{s}} \ln\left[1 - \frac{1}{b_{\mathrm{m}}}\right] \quad (3)$$

where $b_{\mathrm{m}} = \frac{1}{M}\sum_{\mathrm{i}=1}^{\mathrm{M}} b_{\mathrm{i}}$, f_{s} is the signal frequency (Hz), and b_{i} is the number of sequential pairs of points in the timewise heat flux response signal. For the analysis of the collected experimental measurements, the selected initial pair of points was the starting pair. Then, the following pair is selected after a length

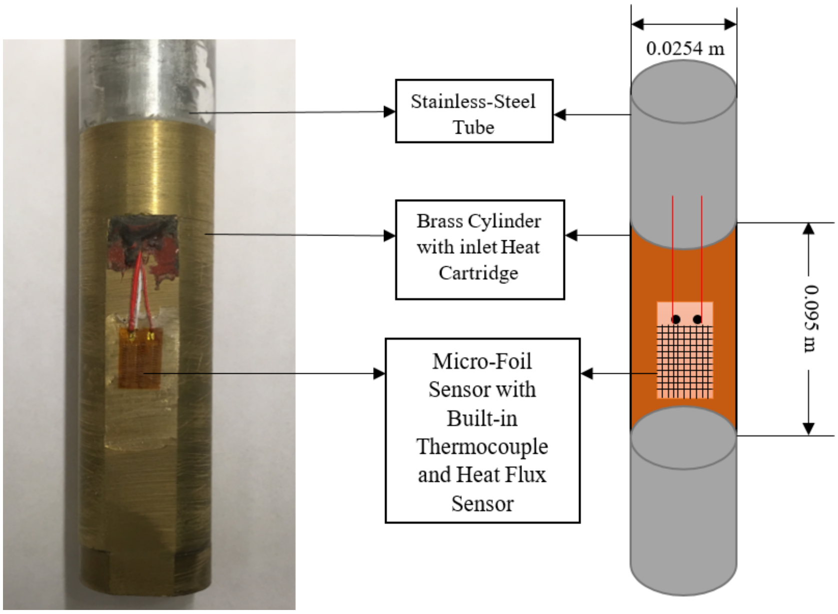

Figure 3. Photo and schematic of the heat transfer probe.

of l_o (maximum interpoint distance); l_o is estimated as $l_o = 3ADD$, where ADD is the average absolute deviation of the timewise signal. Further details regarding the application of the maximum likelihood method to calculate the KW have been reported in the literature and can be found in Schouten et al. [31]. Toukan et al. [40] developed the algorithm and its program in our Multiphase Reactors Engineering and Applications Laboratory (mReal). More details about Kolmogorov entropy's calculation on our FB systems can be found in Taofeeq and Al-Dahhan [6, 8].

5 Results and Discussion

The experiments were conducted at a wide range of superficial gas velocities to cover the operating condition of different flow regimes (fixed-bed, bubbling, slugging, and turbulent-flow regime), as indicated by Taofeeq and Al-Dahhan [8]. The experiments exhibited good reproducibility when comparing the measured heat flux voltage signals measured in the three repetitions on each tested condition. The result data values were almost identical in each repetition with differences below 5 %. The five repetitions are also allowed to determine the error bars shown in the following results figures.

5.1 Flow Regime Transitions

Figs. 4 and 5 illustrate the results of the standard deviation and KE obtained by analyzing the measured time series of the heat flux through the tested wide range of superficial gas inlet velocities, from 0.35 to 1.1 m s^{-1}. A maximum local value of the standard deviation indicates a transition velocity, as reported by Johnson et al. [26] and Van Ommen et al. [29], while for the KE analysis, a local minimum of the heat flux oscillation indicates a transition velocity [32, 34]. In other words, the KE increase when raising the superficial gas inlet velocity implies that the system disorder or the chaotic behavior of the system is incrementing. KE will reach a maximum local value, which indicates an unstable flow regime or a transition regime between the different flow regimes. With a further increase of the inlet velocity, the KE decreases to a local minimum, which implies that the gas-solid interactions are more organized.

As indicated in Figs. 4 and 5, four different flow regimes have been identified by both methods of heat flux oscillations analysis (fixed bed, bubbling regime, slugging regime, and turbulent regime). These flow regimes are separated by three transition velocities: minimum fluidized velocity (U_{mf}), which also corresponds to the minimum bubbling velocity (U_{mb}), then the minimum slugging velocity (U_{slug}), and the turbulent transition velocity (U_c). For Geldart B-type solid particles, the minimum fluidization velocity is equal to the minimum bubbling. However, in other kinds of particles, such as Geldart A type, these two transition velocities are different [33].

Fig. 5 shows that the KE tends to rise when the superficial gas inlet velocity increases. Such tendency indicates an increment in the chaotic and disordered gas-solid interaction phenomena, which is expected. With higher gas flow rate, more vigorous gas-solid interactions are expected. This tendency of the KE to increase is disrupted by the local minimum values at the transition points. In such local minimum points, the gas-solid flow patterns are found to be more ordered.

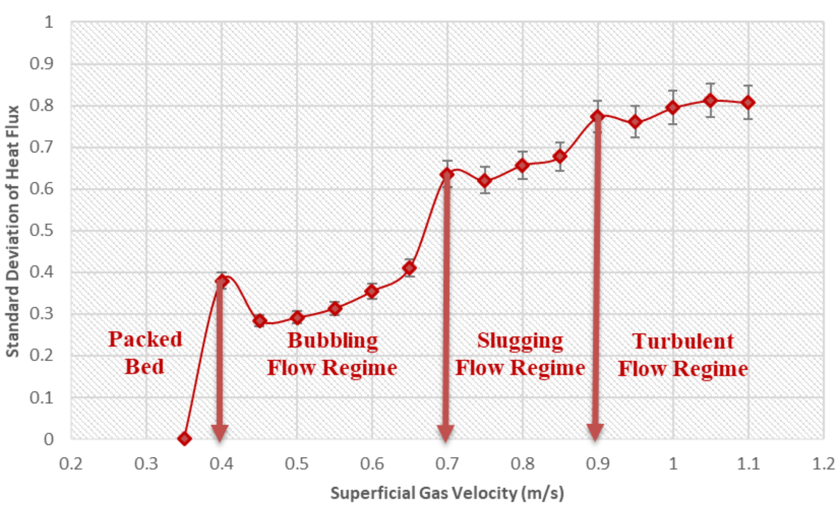

Figure 4. Standard deviation of heat flux oscillations vs superficial gas velocity.

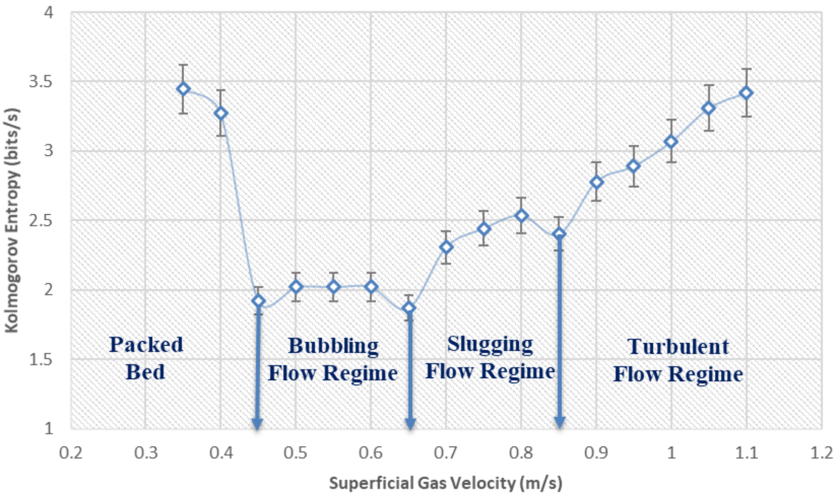

Figure 5. Kolmogorov entropy of heat flux oscillations vs superficial gas velocity.

Figs. 4 and 5 demonstrate the ability of both of the used analysis methods, i.e., standard deviation and KE, for identifying different flow regimes and the transition velocities from the data of heat flux oscillations. Furthermore, it should be noted that the results obtained by both methods are in good agreement with the measurements gained in our previous contribution analyzing the pressure fluctuation signals measured by a differential pressure transducer [18]. The transition velocities within the range for each flow regime for the two data analysis methods and the comparison of present transition velocities with the work of Taofeeq and Al-Dahhan [8] are listed in Tab. 1.

It is clearly shown in Tab. 1 that the current data are in good agreement with the work done by analyzing the pressure fluctuation. This was expected, as the same operating conditions and design parameters were used. These results show that there is no effect of the used internal with built-in heat transfer probe on the flow pattern and transition velocities since the work of Taofeeq and Al-Dahhan [8] was performed in FBs without the presence of internals. Therefore, the existence of a single internal does not affect the hydrodynamics of the system and its flow regime transitions.

According to Nedeltchev et al. [32], most of the industrial applications of FBs are operated at bubbling or at turbulent flow regimes. Hence, it is important to identify the two transition velocities between these regimes, i.e., the minimum fluidized velocity (U_{mf}) and transition velocity (U_c). The proposed method of analyzing the heat flux signals allowed to identify both velocities by different analysis methods. For verification of the determined transition velocities in the experimentally studied FB, correlations found in reported literature were used to calculate such transition velocities, and their predictions were compared against our experimentally determined values. The comparison of these predictions is presented in Tabs. 2 and 3.

It is worth mentioning that the selection of these correlations from the literature has been based on the recommendation of Arnaldos and Casal [35], in which these correlations are considered highly accurate for predicting U_{mf} and U_c for Geldart B particles. As indicated in Tabs. 2 and 3, most of the transition velocities are in good agreement with the values predicted by the correlations available in the literature.

5.2 Heat Flux Oscillations

The heat flux oscillations at different flow regimes are displayed in Fig. 6. Four different superficial gas inlet velocities were selected for each flow regime (0.35-fixed bed, 0.55-bubbling, 0.75-slugging, and 0.95-turbulent $m\,s^{-1}$). It is clearly shown that the oscillation of heat flux voltage signal increase when the superficial gas inlet velocity is increased. Such

Table 1. Transition velocities and the superficial gas velocity within the range of each flow regime for both types of data analysis and the comparison with the work of Taofeeq and Al-Dahhan [8].

Conditions	Present work		Work of Taofeeq and Al-Dahhan [8]		% Relative error with respect to [8]	
Data analysis method	SD	KE	SD	KE	SD	KE
Minimum fluidized velocity U_{mf} [$m\,s^{-1}$]	0.4	0.45	0.4	0.4	0	11.11
Minimum slugging velocity U_{slug} [$m\,s^{-1}$]	0.7	0.65	0.7	0.65	0	0
Transition velocity U_c [$m\,s^{-1}$]	0.9	0.85	0.95	0.95	5.26	10.52
Packed-bed velocity range [$m\,s^{-1}$]	≤ 0.4	≤ 0.45	≤ 0.4	≤ 0.4	11.11	0
Superficial gas velocity within the range of bubbling regime [$m\,s^{-1}$]	0.4–0.7	0.45–0.65	0.4–0.7	0.4–0.65	0	0
Superficial gas velocity within the range of slugging regime [$m\,s^{-1}$]	0.7–0.9	0.65–0.85	0.7–0.95	0.65–0.95	20	20
Superficial gas velocity within the range of turbulent flow regime [$m\,s^{-1}$]	≥ 0.9	≥ 0.85	≥ 0.95	≥ 0.95	20	0

Table 2. Comparison between minimum fluidized velocity U_{mf} (m s^{-1}) measured by this work and the minimum fluidized velocity predicted from the available correlations in the literature.

Conditions	Minimum fluidized velocity
Data analysis method (SD and KE)	0.4, 0.45
$Re_{mf} = 0.000955Ar^{0.96}$ [36]	0.42
$Re_{mf} = \sqrt{(27.2)^2 + 0.0408Ar} - 27.2$ [37]	0.42
% Relative error of SD and KE with respect to [36]	4.76, 6.67
% Relative error of SD and KE with respect to [37]	4.76, 6.67

Table 3. Comparison between transition velocity U_c (m s^{-1}) measured by this work and that predicted from the available correlations in the literature.

Conditions	Transition velocity
Kolmogorov entropy (KE)	0.85
Standard deviation (SD)	0.9
$\frac{U_c}{\sqrt{gd_p}} = \left[\frac{K_{DF}}{d_p}\frac{(\rho_p - \rho_f)}{\rho_f}\right]^n$ where $n = 0.27$ and $K_{DF} = 0.00367$ (for free bed) [38]	0.86
% Relative error of KE with respect to [38]	1.1
% Relative error of SD with respect to [38]	4.4
$Re_c = 0.57Ar^{0.46}$ [39]	1.01
% Relative error of KE with respect to [39]	15.8
% Relative error of SD with respect to [39]	10.9

behavior is identified for all flow regimes, which is in agreement with the results of other researchers who examined the flow regimes in gas-solid fluidized beds [26, 27, 29]. The mean (μ) and the standard deviation (σ) of the heat flux oscillations were estimated. The mean represents the amplitude, while the standard deviation stands for the frequency of the measured timewise response signals.

Fig. 6 clearly demonstrates that the values of the standard deviation of the heat flux voltage signals rise when increasing the superficial gas inlet velocity (flow regime transfer from one to another). The increment of the standard deviation value with the raising of superficial gas inlet velocity indicates a higher system turbulence and interaction between gas and solids and the wall of the vessel or the immersed surfaces inside the bed [16]. Additionally, the change of heat transfer oscillation signals in terms of amplitude (mean) and frequency (standard deviation) is a function of system hydrodynamics such as bubble and solids characteristics inside the bed. Hence, increasing the system oscillation would improve the local and overall heat

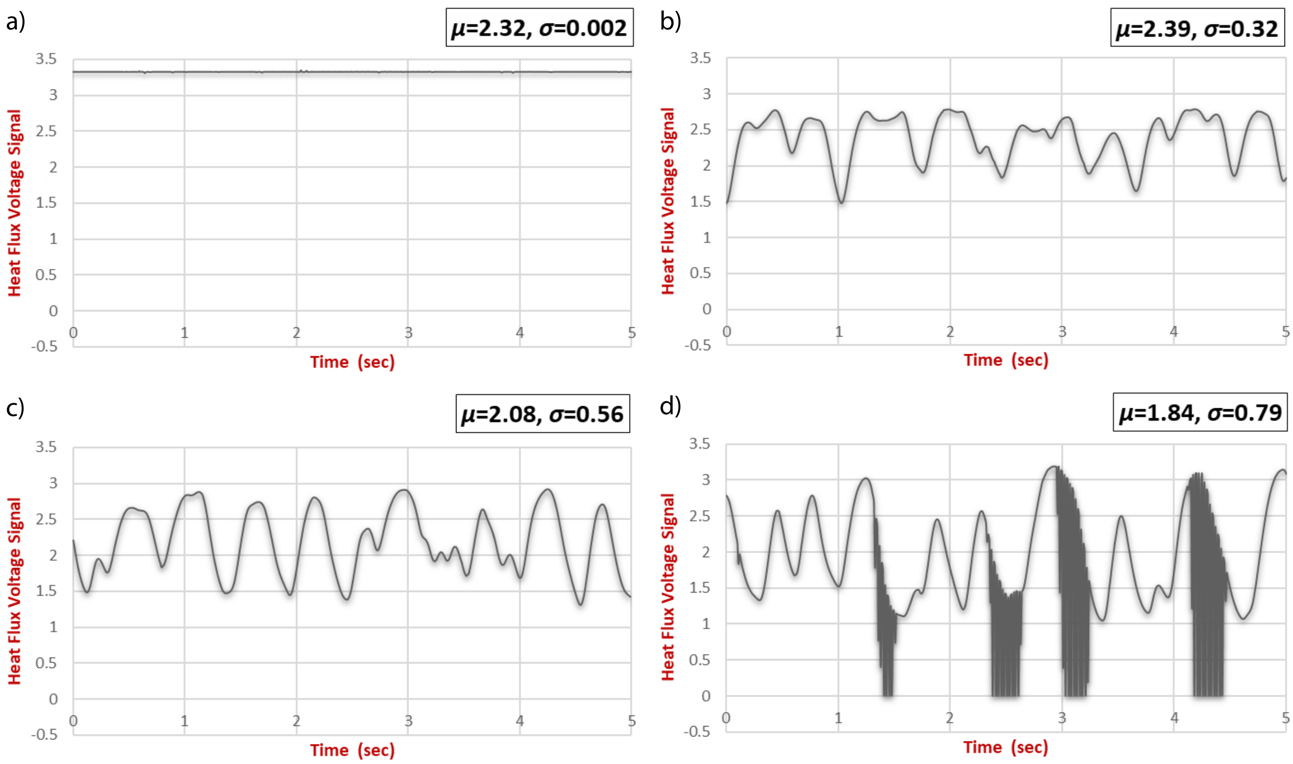

Figure 6. Heat flux signals at different flow regimes. (a) Heat flux signal at a gas velocity of 0.35 m s^{-1} (packed bed flow regime), (b) heat flux signal at a gas velocity of 0.55 m s^{-1} (bubbling flow regime), (c) heat flux signal at a gas velocity of 0.75 m s^{-1} (slugging flow regime), (d) heat flux signal at a gas velocity of 0.95 m s^{-1} (turbulent flow regime).

transfer and mass transfer phenomena inside the bed since the heat and mass transfer phenomena highly depend on the solids and bubbles dynamics.

6 Conclusions

The flow regimes and their transition velocities were successfully identified in a lab-scale gas-solid fluidized bed of 0.14 m inside diameter. The experimental data of the micro-foil sensor in terms of the time series of heat flux was analyzed using the standard deviation and Kolmogorov entropy method. Four different flow regimes (fixed bed, bubbling, slugging, and turbulent) were detected with the range of superficial gas velocity used in the present study (0.35–1.1 $m\,s^{-1}$). Correspondingly, the three transition velocities (minimum fluidizing velocity, minimum slugging velocity, and minimum turbulent velocity) were obtained from the two methods of time-series analyses.

The two major transition velocities (minimum fluidizing velocity and minimum turbulent velocity) estimated by the present work were compared with the most used predicated correlations in the literature. A good agreement was obtained between the two values. These results indicate that the analysis of the heat flux signals is a promising technique to identify the flow regime in a fluidized bed in a non-invasive way. Furthermore, given that the micro-foil sensor is flush-mounted on an internal wall, the prediction of the flow regime is based on information of the hydrodynamics of the core region of the fluidized bed, rather than on the measured phenomena in the near-wall regions, such as is the case when using absolute or differential pressure transducers.

Acknowledgment

The authors would like to thank the Multiphase Reactors Engineering and Applications Laboratory (mReal) for funding and support.

The authors have declared no conflict of measurement.

Symbols used

Ar	[–]	Archimedes number of the solid particles
d_p	[µm]	particle mean diameter or average particle diameter
g	[$m\,s^{-2}$]	acceleration gravity
N	[–]	total number of data points
Re_c	[–]	Reynolds number of solid particles at transition fluidized velocity (U_c)
Re_{mf}	[–]	Reynolds number of the solid particles at minimum fluidized velocity (U_{mf})
U_c	[$m\,s^{-1}$]	transition velocity or turbulent transition velocity
U_{mb}	[$m\,s^{-1}$]	minimum bubbling velocity
U_{mf}	[$m\,s^{-1}$]	minimum fluidization velocity
U_{slug}	[$m\,s^{-1}$]	minimum slugging velocity

Greek letters

ρ	[$kg\,m^{-3}$]	density
ρ_f	[$kg\,m^{-3}$]	fluid density
ρ_p	[$kg\,m^{-3}$]	solid particle density or solid density
φ	[–]	sphericity factor

Sub- and superscripts

c	minimum turbulent fluidization
f	fluid
mb	minimum bubbling
mf	minimum fluidization
p	particle
slug	minimum slugging

Abbreviations

KE	Kolmogorov entropy
SD	standard deviation

References

[1] K. Dubrawski, S. Tebianian, H. T. Bi, J. Chaouki, N. Ellis, R. Gerspacher, R. Jafari, A. Kantzas, C. Lim, G. S. Patience, T. Pugsley, M. Z. Qi, J. X. Zhu, J. R. Grace, Traveling column for comparison of invasive and non-invasive fluidization voidage measurement techniques, *Powder Technol.* **2013**, *235*, 203–220. DOI: https://doi.org/10.1016/j.powtec.2012.10.031

[2] M. Rüdisüli, T. J. Schildhauer, S. M. A. Biollaz, J. R. Van Ommen, Scale-up of bubbling fluidized bed reactors – A review, *Powder Technol.* **2012**, *217*, 21–38. DOI: https://doi.org/10.1016/j.powtec.2011.10.004

[3] J. M. Matsen, Scale-up of fluidized bed processes: Principle and practice, *Powder Technol.* **1996**, *88*, 237–244. DOI: https://doi.org/10.1016/S0032-5910(96)03126-9

[4] M. Rüdisüli, T. J. Schildhauer, S. M. A. Biollaz, J. R. van Ommen, Monte Carlo simulation of the bubble size distribution in a fluidized bed with intrusive probes, *Int. J. Multiphase Flow* **2012**, *44*, 1–14. DOI: https://doi.org/10.1016/j.ijmultiphaseflow.2012.03.009

[5] M. Rüdisüli, T. J. Schildhauer, S. M. A. Biollaz, J. R. Van Ommen, Bubble characterization in a fluidized bed with vertical tubes, *Ind. Eng. Chem. Res.* **2012**, *51*, 4748–4758. DOI: https://doi.org/10.1021/ie2022306

[6] H. Taofeeq, Impact of Vertical Internals on the Hydrodynamics and Heat Transfer Coefficient in a Gas-Solid Fluidized Bed, *Ph.D. Thesis*, Missouri University of Science and Technology, Rolla, MO **2017**.

[7] S. Roy, H. J. Pant, S. Roy, Solids flow pattern in cold flow mockup of fluidized bed gasifier, *Chem. Eng. Sci.* **2019**, *210*, 115225. DOI: https://doi.org/10.1016/j.ces.2019.115225

[8] H. Taofeeq, M. Al-Dahhan, Flow regimes in gas-solid fluidized bed with vertical internals, *Chem. Eng. Res. Des.* **2018**, *138*, 87–104. DOI: https://doi.org/10.1016/j.cherd.2018.07.019

[9] L. Kalo, H. J. Pant, M. C. Cassanello, R. K. Upadhyay, Time series analysis of a binary gas-solid conical fluidized bed using radioactive particle tracking (RPT) technique data,

Chem. Eng. J. **2018**, *377*, 119807. DOI: https://doi.org/10.1016/j.cej.2018.08.193

[10] Y. Zhou, L. Yang, Y. Lu, X. Hu, X. Luo, H. Chen, Flow regime identification in gas-solid two-phase fluidization via acoustic emission technique, *Chem. Eng. J.* **2018**, *334*, 1484–1492. DOI: https://doi.org/10.1016/j.cej.2017.11.050

[11] S. Hamidifard, A. Bahramian, M. Rasteh, Mesh sensitivity analysis on hydrodynamics behavior of a fluidized bed containing silver oxide nanoparticle agglomerates: Transition from bubbling to slugging and turbulent flow regimes, *Powder Technol.* **2018**, *331*, 28–40. DOI: https://doi.org/10.1016/j.powtec.2018.03.002

[12] Q. Zhu, H. Li, Q. Zhu, Q. Huang, Comparing flow regime transition of magnetized fluidized bed with Geldart-B particles between magnetization-FIRST and -LAST operation modes, *Chem. Eng. J.* **2019**, *360*, 686–700. DOI: https://doi.org/10.1016/j.cej.2018.12.053

[13] S. Boonprasop, B. Chalermsinsuwan, P. Piumsomboon, Circulating turbulent fluidized bed regime on flow regime diagram, *Powder Technol.* **2019**, *350*, 146–153. DOI: https://doi.org/10.1016/j.powtec.2019.03.047

[14] Y. Yang, L. He, J. Sun, Z. Huang, J. Wang, Y. Yang, C. Huang, Z. Huang, Measurement and analysis of flow regimes transition by acoustic and electrostatic signals in vertical pneumatic conveying, *Powder Technol.* **2019**, *352*, 283–293. DOI: https://doi.org/10.1016/j.powtec.2019.04.024

[15] H. Taofeeq, M. H. Al-Dahhan, Effect of vertical internals on the pressure drop in a gas-solid fluidized bed, *Can. J. Chem. Eng.* **2018**, *96*, 2185–2205. DOI: https://doi.org/10.1002/cjce.23299

[16] H. Taofeeq, M. Al-Dahhan, The impact of vertical internals array on the key hydrodynamic parameters in a gas-solid fluidized bed using an advance optical fiber probe, *Adv. Powder Technol.* **2018**, *29*, 2548–2567. DOI: https://doi.org/10.1016/j.apt.2018.07.008

[17] H. Taofeeq, S. Aradhya, J. Shao, M. Al-Dahhan, Advance optical fiber probe for simultaneous measurements of solids holdup and particles velocity using simple calibration methods for gas-solid fluidization systems, *Flow Meas. Instrum.* **2018**, *63*, 18–32. DOI: https://doi.org/10.1016/j.flowmeasinst.2018.07.001

[18] H. Taofeeq, M. Al-Dahhan, Comparison between the new mechanistic and the chaos scale-up methods for gas-solid fluidized beds, *Chin. J. Chem. Eng.* **2018**, *26*, 1401–1411. DOI: https://doi.org/10.1016/j.cjche.2018.03.022

[19] H. Taofeeq, M. Al-Dahhan, Heat transfer and hydrodynamics in a gas-solid fluidized bed with vertical immersed internals, *Int. J. Heat Mass Transfer* **2018**, *122*, 229–251. DOI: https://doi.org/10.1016/j.ijheatmasstransfer.2018.01.093

[20] C. Wu, M. H. Al-Dahhan, A. Prakash, Heat transfer coefficients in a high-pressure bubble column, *Chem. Eng. Sci.* **2007**, *62*, 140–147. DOI: https://doi.org/10.1016/j.ces.2006.08.016

[21] R. S. Abdulmohsin, B. A. Abid, M. H. Al-Dahhan, Heat transfer study in a pilot-plant scale bubble column, *Chem. Eng. Res. Des.* **2011**, *89*, 78–84. DOI: https://doi.org/10.1016/j.cherd.2010.04.019

[22] R. S. Abdulmohsin, M. H. Al-Dahhan, Impact of internals on the heat-transfer coefficient in a bubble column, *Ind. Eng. Chem. Res.* **2012**, *51*, 2874–2881. DOI: https://doi.org/10.1021/ie2018096

[23] I. A. S. Abdallah, Experimental study of natural convection heat transfer and gaseous dynamics from dual-channel circulation loop, *Ph.D. Thesis*, Missouri University of Science and Technology, Rolla, MO **2017**.

[24] K. Pisters, A. Prakash, Investigations of axial and radial variations of heat transfer coefficient in bubbling fluidized bed with fast response probe, *Powder Technol.* **2011**, *207*, 224–231. DOI: https://doi.org/10.1016/j.powtec.2010.11.003

[25] S. Uribe, N. Zouli, M. E. Cordero, M. Al-Dahhan, Development and validation of a mathematical model to predict the thermal behaviour of nanofluids, *Heat Mass Transfer* **2021**, *57*, 93–110. DOI: https://doi.org/10.1007/s00231-020-02927-5

[26] F. Johnson, R. C. Zijerveld, J. C. Schouten, C. M. van den Bleek, B. Leckner, Characterization of fluidization regimes by time-series analysis of pressure fluctuations, *Int. J. Multiphase Flow* **2000**, *26*, 663–715. DOI: https://doi.org/10.1103/PhysRevE.49.126

[27] J. Saayman, W. Nicol, J. R. Van Ommen, R. F. Mudde, Fast X-ray tomography for the quantification of the bubbling-, turbulent- and fast fluidization-flow regimes and void structures, *Chem. Eng. J.* **2013**, *234*, 437–447. DOI: https://doi.org/10.1016/j.cej.2013.09.008

[28] G. Qiu, J. Ye, H. Wang, W. Yang, Investigation of flow hydrodynamics and regime transition in a gas-solids fluidized bed with different riser diameters, *Chem. Eng. Sci.* **2014**, *116*, 195–207. DOI: https://doi.org/10.1016/j.ces.2014.05.006

[29] J. R. Van Ommen, S. Sasic, J. Van der Schaaf, S. Gheorghiu, F. Johnsson, M. O. Coppens, Time-series analysis of pressure fluctuations in gas-solid fluidized beds – A review, *Int. J. Multiphase Flow* **2011**, *37*, 403–428. DOI: https://doi.org/10.1016/j.ijmultiphaseflow.2010.12.007

[30] J. C. Schouten, F. Takens, C. M. Van Den Bleek, Estimation of the dimension of a noisy attractor, *Phys. Rev. E* **1994**, *50*, 1851–1861. DOI: https://doi.org/10.1103/PhysRevE.50.1851

[31] J. C. Schouten, F. Takens, C. M. Van Den Bleek, Maximum-likelihood estimation of the entropy of an attractor, *Phys. Rev. E* **1994**, *49*, 126–129. DOI: https://doi.org/10.1103/PhysRevE.49.126

[32] S. Nedeltchev, F. Ahmed, M. Al-Dahhan, A new method for flow regime identification in a fluidized bed based on gamma-ray densitometry and information entropy, *J. Chem. Eng. Jpn.* **2012**, *45*, 197–205. DOI: https://doi.org/10.1252/jcej.11we189

[33] S. Nedeltchev, S. Aradhya, F. Zaid, M. Al-Dahhan, Flow regime identification in three multiphase reactors based on Kolmogorov entropies derived from gauge pressure fluctuations, *J. Chem. Eng. Jpn.* **2012**, *45*, 757–764. DOI: https://doi.org/10.1252/jcej.12we075

[34] S. Nedeltchev, New methods for flow regime identification in bubble columns and fluidized beds, *Chem. Eng. Sci.* **2015**, *137*, 436–446. DOI: https://doi.org/10.1016/j.ces.2015.06.054

[35] J. Arnaldos, J. Casal, Prediction of transition velocities and hydrodynamical regimes in fluidized beds, *Powder Technol.* **1996**, *86*, 285–298. DOI: https://doi.org/10.1016/0032-5910(95)03054-9

[36] S. Shaul, E. Rabinovich, H. Kalman, Generalized flow regime diagram of fluidized beds based on the height to bed diameter ratio, *Powder Technol.* **2012**, *228*, 264–271. DOI: https://doi.org/10.1016/j.powtec.2012.05.029

[37] H. T. Bi, J. R. Grace, Flow regime diagrams for gas-solid fluidization and upward transport, *Int. J. Multiphase Flow* **1995**, *21*, 1229–1236. DOI: https://doi.org/10.1016/0301-9322(95)00037-X

[38] Y. Jin, Z. Yu, Z. Wang, P. Cai, A criterion for transition from bubbling to turbulent fluidization, *Fluid* **1986**, *5*, 289–296.

[39] K. S. Lim, J. X. Zhu, J. R. Grace, Hydrodynamics of gas-solid fluidization, *Int. J. Multiphase Flow* **1995**, *21*, 141–193.

[40] A. Toukan, V. Alexander, H. AlBazzaz, M. H. Al-Dahhan, Identification of flow regime in a cocurrent gas-liquid upflow moving packed bed reactor using gamma ray densitometry, *Chem. Eng. Sci.* **2017**, *168*, 380–390. DOI: https://doi.org/10.1016/j.ces.2017.04.028

